Earth and Space Science

RESEARCH ARTICLE
10.1029/2023EA003045

Special Section:
The Mars Perseverance Rover Jezero Crater Floor Campaign

# A High-Resolution Digital Terrain Model Mosaic of the Mars 2020 Perseverance Rover Landing Site at Jezero Crater

**Yu Tao[1,2], Sebastian H. G. Walter[1], Jan-Peter Muller[2], Yaowen Luo[1,3], and Siting Xiong[4]**

[1]Planetary Sciences and Remote Sensing Group, Department of Earth Sciences, Freie Universität Berlin, Berlin, Germany, [2]Mullard Space Science Laboratory, Department of Space and Climate Physics, University College London, Surrey, UK, [3]Chinese Antarctic Center of Surveying and Mapping, Wuhan University, Wuhan, China, [4]Guangdong Laboratory of Artificial Intelligence and Digital Economy, Shenzhen, China

**Key Points:**

- We demonstrate the capabilities of a published MADNet monocular height estimation network in producing a refined digital terrain model mosaic at 50 cm/pixel resolution for the Mars 2020 Perseverance rover landing site in Jezero crater on Mars
- The resultant 50 cm/pixel digital terrain model mosaic demonstrates significant improvements in effective resolution and artifact elimination compared to the publicly available Mars 2020 Terrain Relative Navigation TRN High-Resolution Imaging Science Experiment digital terrain model
- The resultant digital terrain model mosaic has been made publicly available at http://dx.doi.org/10.17169/refubium-38359

**Correspondence to:**
Y. Tao,
yu.tao@fu-berlin.de

**Citation:**
Tao, Y., Walter, S. H. G., Muller, J.-P., Luo, Y., & Xiong, S. (2023). A high-resolution digital terrain model mosaic of the Mars 2020 Perseverance rover landing site at Jezero crater. *Earth and Space Science*, *10*, e2023EA003045. https://doi.org/10.1029/2023EA003045

Received 16 MAY 2023
Accepted 21 SEP 2023

**Author Contributions:**
**Conceptualization:** Yu Tao, Sebastian H. G. Walter, Jan-Peter Muller
**Data curation:** Yu Tao, Sebastian H. G. Walter, Yaowen Luo



**Abstract** We demonstrate the capabilities of a published MADNet monocular height estimation network in producing a refined digital terrain model (DTM) mosaic at 50 cm/pixel resolution for the Mars 2020 Perseverance rover landing site in Jezero crater on Mars. Our approach utilizes the publicly available Mars 2020 Terrain Relative Navigation (TRN) High-Resolution Imaging Science Experiment (HiRISE) Digital Terrain Model (DTM) mosaic, which was originally created by the United States Geological Survey (USGS) Astrogeology Science Centre. Our resultant HiRISE MADNet DTM mosaic is strictly matched with the original HiRISE TRN DTM and orthoimage mosaics. These mosaics are themselves co-aligned with the USGS TRN Context Camera (CTX) based DTM and orthoimage mosaics, as well as the ESA/DLR/FUB (European Space Agency/German Aerospace Center/Free University Berlin) High Resolution Stereo Camera (HRSC) level 5 DTM and orthoimage mosaics. In this paper, we provide a brief description of the technical details, and present both visual and quantitative assessments of the refined MADNet HiRISE Jezero DTM mosaic product. This DTM product is now publicly available at http://dx.doi.org/10.17169/refubium-38359.

## 1. Introduction

Accurate three-dimensional (3D) mapping of the Martian surface is critical for geological characterization, safe landing, planning, and engineering operations of robotic missions and future human explorations. Over the past 20 years, there has been a revolution in 3D mapping of the Martian surface since the successful launching of the ESA and NASA high-resolution imaging instruments. The spatial resolution of the available Mars 3D models has increased from hundreds of meters from the Mars Orbiter Laser Altimeter (MOLA) (Smith et al., 2001, p. 2. Neumann et al., 2001) to tens of meters from the Mars Express's High Resolution Stereo Camera (HRSC) (Gwinner et al., 2009; Neukum & Jaumann, 2004), and subsequently to meters and centimeters scale from the Mars Reconnaissance Orbiter (MRO)'s Context Camera (CTX) (Malin et al., 2007; Tao et al., 2018) and High-Resolution Imaging Science Experiment (HiRISE) (McEwen et al., 2007; Tao et al., 2021a, 2022).

The NASA Mars 2020 mission required highly accurate 3D models of the Martian surface to support safe landing, engineering operations, and the geological characterization of the landing site at Jezero crater (Mangold et al., 2020; Stack et al., 2020). In preparation for this mission, the United States Geological Survey (USGS) produced digital terrain model (DTM) and orthorectified image (ORI) mosaics using the MRO CTX and HiRISE stereo images for the new onboard landing system, called the Lander Vision System (LVS) and Terrain Relative Navigation (TRN) (Fergason et al., 2020). These products were carefully co-registered to accurately align the output DTMs (Fergason et al., 2020) with the ESA/DLR/FUB (European Space Agency/German Aerospace Centre/Free University Berlin) HRSC level 5 ORI and DTM mosaics, which are internationally recognized as the most geodetically accurate global base map with respect to MOLA to date (Gwinner et al., 2016; Sidiropoulos et al., 2018).

However, the 1 m/pixel Mars 2020 TRN HiRISE DTM Mosaic (for brevity, hereafter referred to as HiRISE TRN DTM) from USGS has limitations in terms of fine-scale features such as dune textures, smaller craters (diameters less than 10 m), and rocks (diameter less than 5 m), as well as artifacts such as striping, contouring, and interpolated areas (refer to Section 3.2). In this work, we address these limitations and improve the quality and accuracy of fine-scale features using the proposed MADNet (Tao et al., 2021a) based DTM refinement processing pipeline. MADNet is a deep learning model designed for monocular height estimation from single images, with a particular focus on Mars orbital imagery. The network was initially demonstrated to create DTMs

**Formal analysis:** Yu Tao, Sebastian H. G. Walter, Yaowen Luo
**Funding acquisition:** Sebastian H. G. Walter, Jan-Peter Muller
**Investigation:** Yu Tao, Sebastian H. G. Walter, Jan-Peter Muller, Siting Xiong
**Methodology:** Yu Tao, Jan-Peter Muller, Siting Xiong
**Project Administration:** Sebastian H. G. Walter
**Resources:** Yu Tao, Sebastian H. G. Walter, Jan-Peter Muller, Yaowen Luo
**Software:** Yu Tao, Siting Xiong
**Supervision:** Sebastian H. G. Walter
**Validation:** Yu Tao, Sebastian H. G. Walter, Yaowen Luo
**Visualization:** Yu Tao, Yaowen Luo, Siting Xiong
**Writing – original draft:** Yu Tao
**Writing – review & editing:** Yu Tao, Sebastian H. G. Walter, Jan-Peter Muller, Yaowen Luo, Siting Xiong

from the ExoMars Trace Gas Orbiter (TGO) Color and Stereo Surface Imaging System (CaSSIS) images (Tao et al., 2021a), and subsequently extended to produce high-quality DTM products from HiRISE, CTX and HRSC images (Tao et al., 2021b, 2021c). In this work, we propose a light-weight DTM refinement processing chain using the pre-trained MADNet model as a backbone to refine the HiRISE TRN DTM product.

We use the 25 cm/pixel Mars 2020 TRN HiRISE ORI Mosaic (hereafter referred to as HiRISE TRN ORI) from USGS as an input for the inference of high-frequency topography. Subsequently, we use the 1 m/pixel HiRISE TRN DTM to retrieve the low-frequency topography of the final resultant 50 cm/pixel MADNet HiRISE Jezero DTM. This DTM product is now publicly available at http://dx.doi.org/10.17169/refubium-38359. We present detailed comparisons between the resultant MADNet HiRISE Jezero DTM and the originating HiRISE TRN DTM, leading us to believe that the published 50 cm/pixel MADNet HiRISE Jezero DTM is the most accurate 3D model of the Mars 2020 landing site at Jezero crater to date.

## 2. Materials and Methods

### 2.1. Existing HiRISE, CTX, and HRSC DTMs and ORIs

Previous efforts have been undertaken by NASA/USGS/JPL and ESA/DLR/FUB to produce HiRISE, CTX, and HRSC DTMs and ORIs that cover the Jezero crater. In particular, the HiRISE TRN DTM was produced using the commercial SOCET SET® software following a standard USGS-ISIS (Integrated Software for Imagers and Spectrometers) process for generating HiRISE DTMs. This involved manually designating tie-points, running relative bundle adjustments, extracting elevation information through stereo image matching, densifying the control network, extracting single-strip DTMs at a resolution of 1 m/pixel. The NASA Ames Stereo Pipeline (ASP) was then utilized for point-cloud co-alignment and DTM mosaicing (Fergason et al., 2020). The HiRISE TRN ORI and DTM mosaics have been co-aligned with the Mars 2020 TRN CTX DTM and ORI mosaics, which themselves are co-aligned with the HRSC Mars Chart 30 (hereafter referred to as HMC30) level 5 DTM and ORI mosaics. The HMC30 DTMs and ORI mosaics were co-aligned with the MOLA global DTM (Gwinner et al., 2009). The MADNet HiRISE Jezero DTM product itself is strictly matching the HiRISE TRN ORI and DTM products pixel-by-pixel as they are used as the direct input and reference, respectively, in the DTM production process. Table 1 provides a summary of the existing relevant data sets over the Jezero crater and their product pages (last assessed on 24 March 2023).

The HiRISE and CTX TRN DTMs and ORI mosaics exhibit superior horizontal and vertical accuracies compared to each other and to the HMC30 MC-13 DTM and ORIs, meeting the requirements for TRN. According to Fergason et al. (2020), the median horizontal and mean vertical differences between the HiRISE and CTX TRN products are 2.1 and 0.4 m, respectively, with 95.4% of the tested feature correspondences having horizontal differences less than 6 m. On a coarser scale, the mean horizontal and vertical differences between the CTX TRN and the HMC30 MC-13 products are 9.6 and 3.8 m, respectively. Comparing the HMC30 MC-13 DTM (specifically, the first of four tiles: HMC_13E10_DA5) to the interpolated MOLA DTM (refer to Table 1), the average vertical differences are 0.161 and 8.618 m, for the entire mosaic and the area covered by the HiRISE TRN DTM, respectively. It should be noted that there also exists another CTX data set by the USGS with a larger extent, called the Mars 2020 Science Investigation CTX DEM Mosaic, which has been extended by adding more CTX orbits which have not been co-aligned to HRSC, but only to the MOLA data set, and for which we observe significant pixel offsets from HRSC.

### 2.2. An Overview of the MADNet Monocular Height Estimation Network

The processing backbone of this work is the deep learning based MADNet monocular height estimation network, developed at University College London (UCL) as described in Tao et al. (2021a). The MADNet network employs a relativistic average Generative Adversarial Network (RaGAN) (Goodfellow et al., 2014; Jolicoeur-Martineau, 2018) and a fully convolutional U-net (Ronneberger et al., 2015) generator network that is constructed using dense convolution (Huang et al., 2017) and up-projection blocks (Laina et al., 2016). The training process of this network involved utilizing a combination of post-processed Planetary Data System (PDS) HiRISE ORIs and DTMs at their effective resolution of 4 m/pixel, and iMars CTX ORIs and DTMs (Tao et al., 2018) at their effective resolution of 36 m/pixel. In the context of DTMs and geospatial image data sets, the term "effective resolution" refers to the actual spatial resolution at which the smallest distinguishable feature can be accurately represented, taking into account factors such as sensor quality, processing techniques, and

**Table 1**
*Summary of the Existing DTM and/or ORI Products Over Jezero Crater*

| Product name | Source | Resolution | Producer | Product page |
|---|---|---|---|---|
| Mars 2020 TRN HiRISE DTM/ORI mosaic | HiRISE | 1 and 25 cm/pixel | NASA/USGS/JPL | https://doi.org/10.5066/P9REJ9JN |
| Mars 2020 TRN CTX DTM/ORI mosaic | CTX | 20 and 6 m/pixel | NASA/USGS/JPL | https://doi.org/10.5066/P9QJDP48 |
| HMC30 HMC_13E10_DA5 level 5 DTM/ORI mosaic | HRSC | 50 and 12.5 m/pixel | ESA/DLR/FUB | https://hrscteam.dlr.de/public/data/HMC30/quads.php?quad=mc13e |
| Mars MGS MOLA DTM 463m v2 | MOLA | 463 m/pixel | MOLA team/USGS | https://astrogeology.usgs.gov/search/map/Mars/GlobalSurveyor/MOLA/Mars_MGS_MOLA_DEM_mosaic_global_463m |

other variables that may affect the clarity of the data. This is distinct from the "nominal resolution," which is the resolution at which the data is sampled or intended to be represented. It should be noted that down-sampling of the training DTMs produced from photogrammetric methods (i.e., from 1 m/pixel into 4 m/pixel for the PDS HiRISE DTMs and from 18 m/pixel into 36 m/pixel for the iMars CTX DTMs) helps to remove high-frequency photogrammetric artifacts and bring their nominal resolution closer to their effective resolution in order to train the network to perform per-pixel image-to-height inference. The loss function for the training process was a weighted combination of gradient loss, Berhu loss (Zwald & Lambert-Lacroix, 2012), and adversarial loss within the RaGAN framework (Tao et al., 2021a).

### 2.3. Overall Processing Chain

The overall process starts with the MADNet image-to-height inference process, which iteratively operates on each small overlapping tile (512 × 512 pixels) that is sliced from the input HiRISE TRN ORI mosaic. Instead of using the coarse-to-fine tiling and inference process as described in Tao et al. (2021a)), we perform the tiling and inference process only at the finest scale of the input image. This is because a photogrammetric DTM of the same image has already been generated and can be directly used to retrieve the low frequency topographic information that is missing from the single-scale tiled image-to-height inference process. Consequently, the multi-scale co-alignment process described in Tao et al. (2021a) is also not necessary for this study. We directly rescale the normalized minimum and maximum relative height values (i.e., 0.0–1.0) of each tiled height output from MADNet to the minimum and maximum height values derived from the corresponding tiles of the reference HiRISE TRN DTM. After converting the relative heights to absolute heights, a lowpass filtered version of the difference map between the reference HiRISE TRN DTM and the rescaled MADNet height map is directly added to the rescaled MADNet height map as the coarse-scale topographic information. These processes are repeated for each tiled height output from MADNet. Finally, the tiled, rescaled, and coarse-scale topography retrieved height outputs are mosaiced to form the initial version of the MADNet HiRISE DTM over Jezero crater. A flow diagram of the overall processing chain is provided in Figure 1.

The resulting DTM is subsequently being checked and refined in multiple iterations to eliminate all identified artifacts and gaps. Examples of these can be found in Section 3.3. In order to eliminate striping artifacts caused

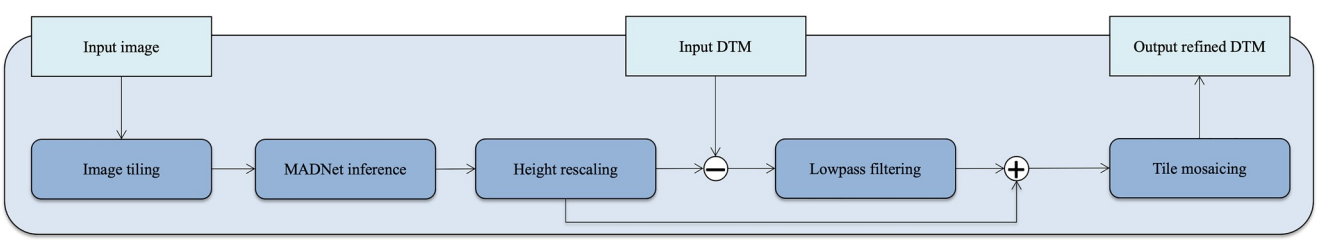


**Figure 1.** Processing chain of the MADNet based DTM refinement workflow.

**Table 2**
*HiRISE Image IDs That Are Used to Improve the HiRISE MADNet DTM Mosaic*

| Blending order | Input HiRISE image IDs |
|---|---|
| 1 | ESP_037119_1985_NORTH_Edited_affine_25cm_Eqc_latTs0_lon0_offNadir.tif |
| 2 | ESP_037818_1990_Edited_affine_25cm_Eqc_latTs0_lon0.tif |
| 3 | ESP_048908_1985_Edited_affine_25cm_Eqc_latTs0_lon0_offNadir.tif |
| 4 | PSP_003798_1985_Edited_affine_25cm_Eqc_latTs0_lon0_offNadir.tif |
| 5 | ESP_046060_1985_Edited_affine_25cm_Eqc_latTs0_lon0_offNadir.tif |
| 6 | JEZ_hirise_soc_006_orthoMosaic_25cm_Eqc_latTs0_lon0_first.tif |

*Note*. The final version of the resultant DTM is blended in the order that is shown on the first column (from front to back).

by the mosaicing and blending process of the HiRISE TRN ORI mosaic, as well as striping artifacts caused by problematic HiRISE images due to poor radiometric de-calibration, we manually select multiple overlapping HiRISE ORIs, use these for another iteration of DTM refinement resulting in refined single-strip HiRISE DTMs, and blend them with the improved versions of the MADNet HiRISE Jezero DTM mosaic. This process is repeated until no further issues are found by visual inspection. The HiRISE image IDs used in this process are listed in Table 2. It should be noted that the single-strip HiRISE images are the co-registered HiRISE images that are published alongside their DTM and ORI mosaics by USGS. They are available from the product pages listed in Table 1.

## 3. Results

### 3.1. An Overview of the Resultant MADNet HiRISE Jezero DTM Mosaic

Figure 2 provides an overview of the 50 cm/pixel MADNet HiRISE Jezero DTM mosaic over the Mars 2020 landing site, which covers the same extent as the original products. The resultant DTM offers significant improvements over the existing product in four main areas: (a) increased effective resolution, allowing for better resolution of fine-scale surface features such as dunes, ripples, small craters, small Transverse Aeolian Ridges (TARs), and rocks; (b) reduced striping artifacts; (c) elimination of matching artifacts (regions of low matching quality); and (d) elimination of interpolation artifacts. Examples for each of these improvements can be found in Section 3.2. While we have made these improvements, we also conducted a thorough check of the MADNet products to identify any remaining issues. Any issues that were found were corrected or refined either by using different processing parameters or by utilizing different repeated input HiRISE images, as described in Section 2.3 and Table 1. These refinements included eliminating small gaps, eliminating striping artifacts caused by brightness/contrast differences of adjacent HiRISE images, and eliminating striping artifacts caused by image artifacts from the original HiRISE data. Examples for each of these refinements can be found in Section 3.3.

### 3.2. Improvements Compared to the Pre-Existing HiRISE TRN DTM Mosaic

In this section, we present examples of the improvements achieved in comparison to the original HiRISE TRN DTM. Figure 3 demonstrates the enhanced effective resolution over various fine-scale surface features, as depicted by shaded relief images of the HiRISE TRN DTM and our MADNet HiRISE Jezero DTM, with the HiRISE TRN ORI mosaic serving as a reference. Figure 3a shows an example of the fine-scale dunes and ripples, while Figure 3b shows two small craters with diameters less than 5 m. Figure 3c shows fine-scale TARs within a shallow crater, and Figure 3d highlights small rocks with lengths less than 3 m. We can observe that the HiRISE TRN DTM mosaic lacks these fine-scale features, whereas the resultant MADNet DTM offers a qualitatively good reconstruction of such features as revealed by visual comparisons with the HiRISE TRN ORI mosaic.

Figure 4 illustrates the improvement in reducing the striping and seamline artifacts identified in the HiRISE TRN DTM. These linear structures appear as local maxima or local minima on the original DTM. All recognizable striping issues have been successfully eliminated in the resultant MADNet DTM.

Figure 5 demonstrates the effectiveness of eliminating the matching artifacts that appeared in the HiRISE TRN DTM. These types of artifacts typically emerge on heavily shaded areas where stereo matching is difficult.

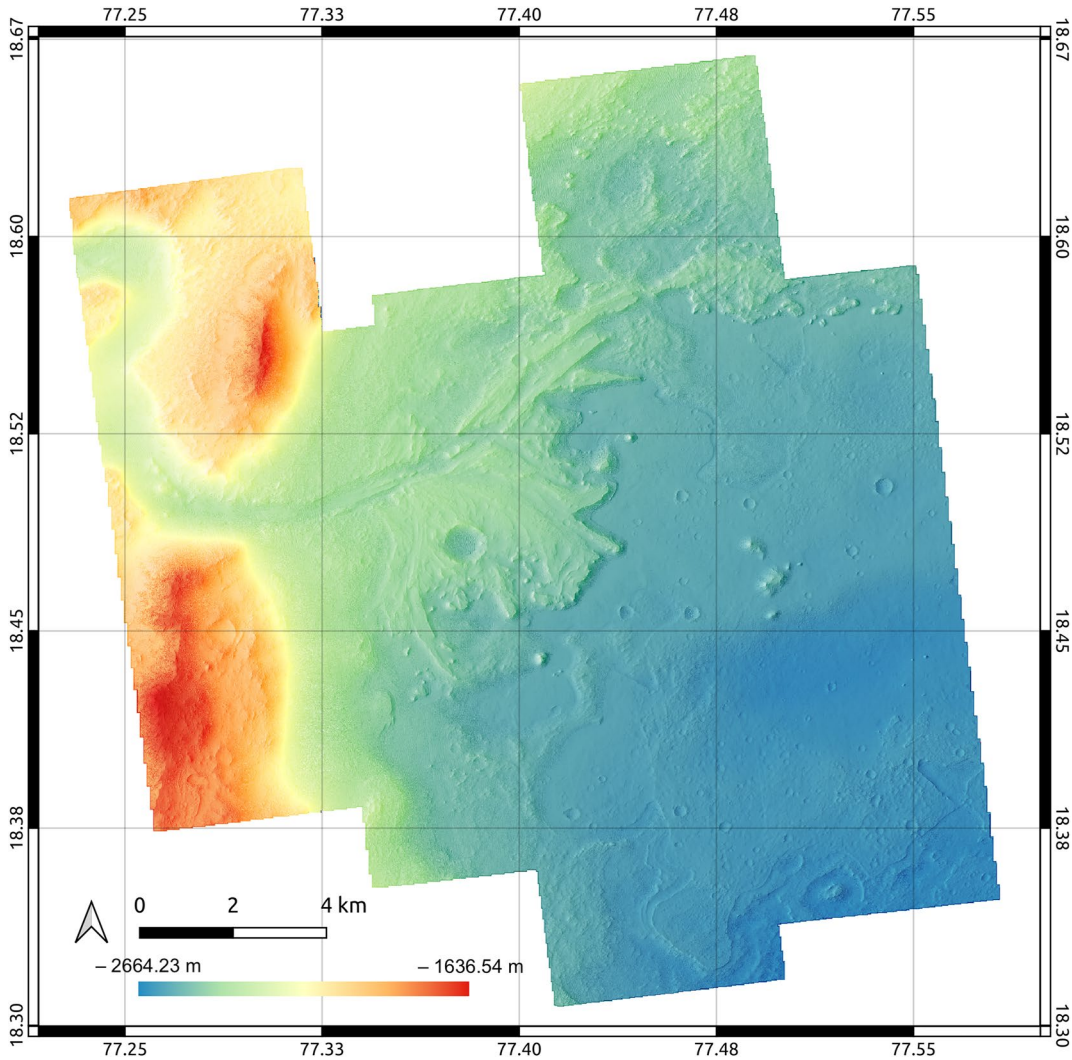


**Figure 2.** An overview of the resultant 50 cm/pixel HiRISE MADNet Jezero DTM over the Mars 2020 landing site, colorized and hill-shaded (azimuth: 275°; altitude: 30°; no vertical exaggeration).

Examples of these are displayed on the shaded floors of the bedrocks in Figure 5a and the shaded slopes of the hill in Figure 5c. Figure 5b shows an example of a medium-sized crater with a diameter of about 100 m that exhibits artifacts inside the crater, such as the small valley near the center, in the HiRISE TRN DTM. Such artifacts do not appear in the resultant MADNet DTM.

The photogrammetric approach used to generate the HiRISE TRN DTM also results in occasional gaps, in particular for areas that fail to match, which are subsequently interpolated based on neighboring topography. Such interpolation artifacts are not shown in the resultant MADNet DTM. Figure 6 shows examples where these interpolation artifacts have been successfully corrected.

### 3.3. Quality Checking and Refinements

After the initial production of the MADNet Jezero DTM, we carefully examined the entire map using shaded relief images and the original HiRISE TRN ORI mosaic for comparison. This scrutiny revealed several new issues in the MADNet version that were absent from the original mosaic. Subsequently, we corrected these issues using different processing parameters or by incorporating different input HiRISE images. The newly introduced issues included occasional gaps, with only three small gaps being found, and new striping artifacts that resulted from the brightness/contrast disparities between neighboring HiRISE images used to generate the input ORI

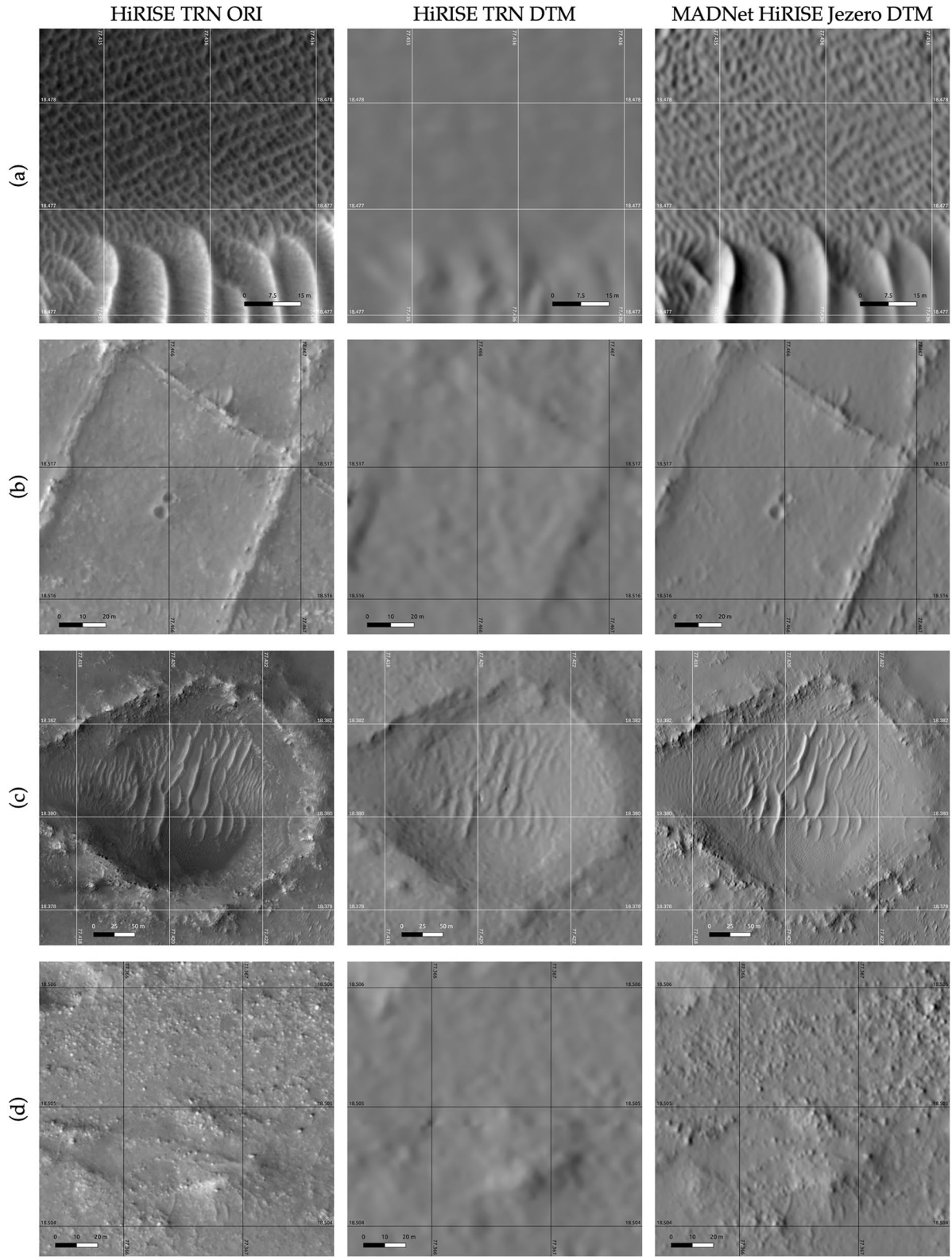


**Figure 3.** Examples of crops of the HiRISE TRN ORI mosaic, shaded relief images (azimuth: 275°; altitude: 30°; vertical exaggeration: (1) of the HiRISE TRN DTM mosaic and the refined MADNet HiRISE Jezero DTM, showing improved effective resolution on the topography of fine-scale surface features.

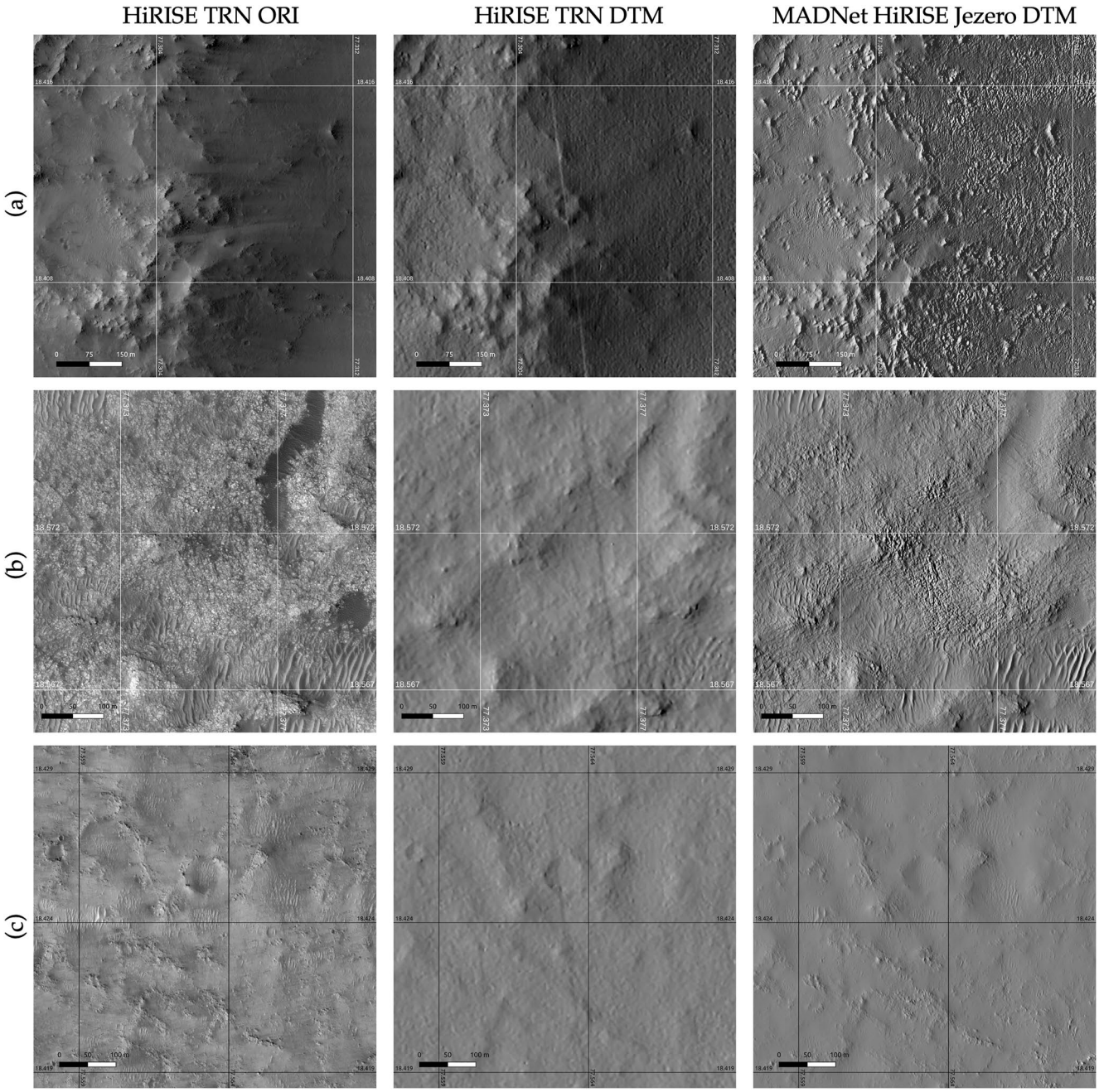


**Figure 4.** Examples of crops of the HiRISE TRN ORI mosaic, shaded relief images (azimuth: 275°; altitude: 30°; vertical exaggeration: (1) of the HiRISE TRN DTM and the refined MADNet HiRISE Jezero DTM, showing the striping artifacts being eliminated.

mosaic. Additionally, new striping artifacts were caused by similar artifacts in the original single-strip HiRISE ORI images. Examples of these issues can be seen in Figures 7, 8, and 9, where we present the initial MADNet HiRISE DTM and the final version of the MADNet HiRISE DTM as shaded relief images, compared to the original HiRISE TRN ORI mosaic. Figure 7 illustrates an issue where some entire tiles were removed during the MADNet processing due to the presence of a few nodata values in the reference DTM. This problem was rectified by reprocessing these tiles using bilinear interpolation and applying a threshold to disregard occasional nodata values before removing the entire tiles. Figure 8 shows an issue where the input HiRISE ORI mosaic exhibits a sharp brightness change between two mosaiced HiRISE ORIs. This issue was eliminated by reprocessing the single-strip HiRISE ORIs (refer to Table 2) that cover the sharp edge of the mosaic, and then blending

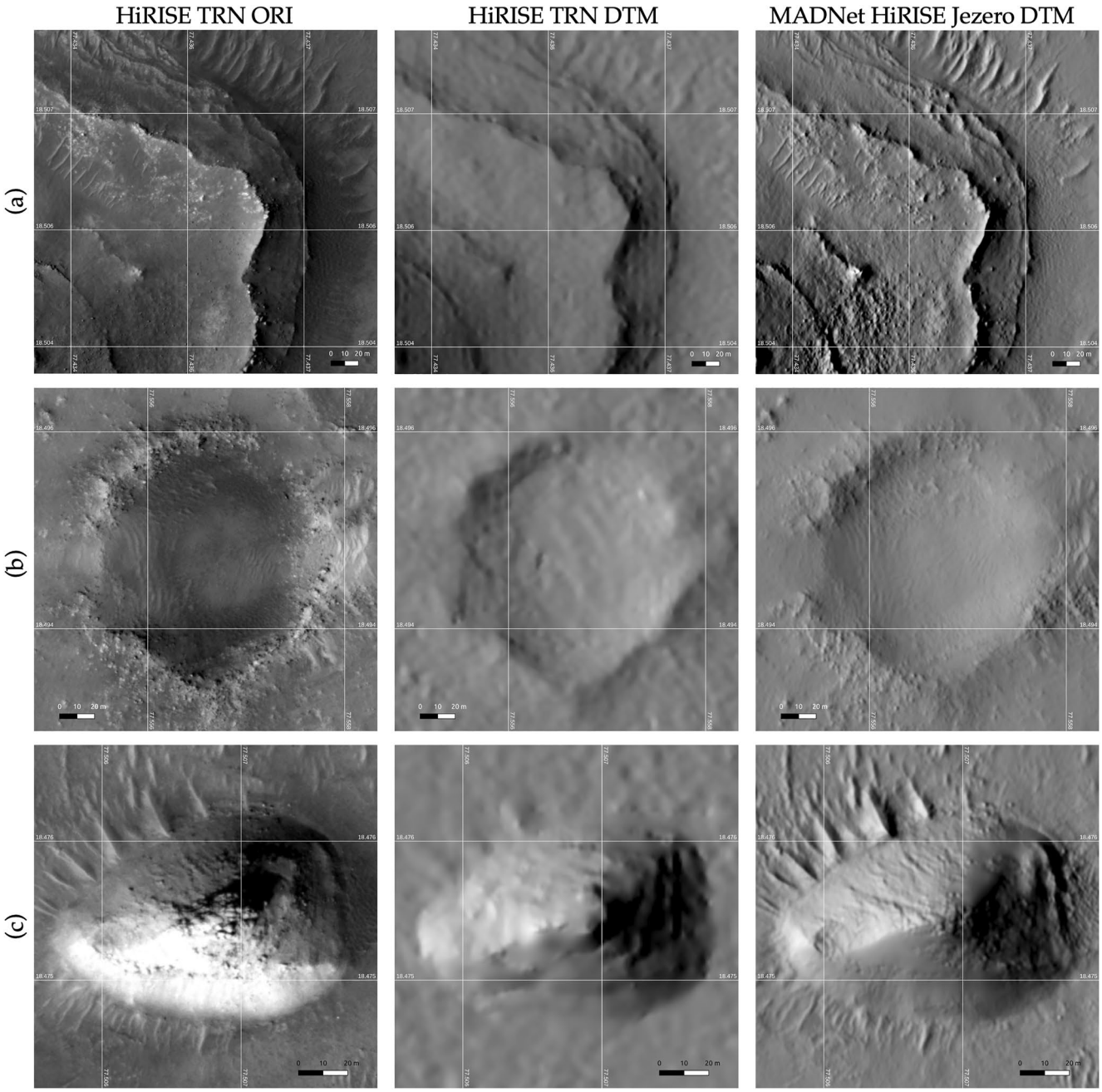


**Figure 5.** Examples of crops of the HiRISE TRN ORI mosaic, shaded relief images (azimuth: 275°; altitude: 30°; vertical exaggeration: (1) of the HiRISE TRN DTM and the refined MADNet HiRISE Jezero DTM, showing improvements on matching artifacts.

the single-strip HiRISE DTMs with the DTM mosaic. Figure 9 reveals the stripping artifacts caused by the same artifacts in the original HiRISE ORIs. In this case, multiple repeated HiRISE ORIs were reprocessed (refer to Table 2), manually cropped along the stripping artifacts, and mosaiced together. This approach was feasible because the stripping artifacts were not located in the exact same position in the different HiRISE ORIs, even though they appeared in similar locations in all of these HiRISE ORIs.

### 3.4. Quantitative Assessments

We conducted quantitative assessments by comparing the resultant 50 cm/pixel MADNet HiRISE DTM mosaic to the 1 m/pixel HiRISE and 20 m/pixel CTX TRN DTMs, as well as to the 50 m/pixel HMC30 MC-13 DTM

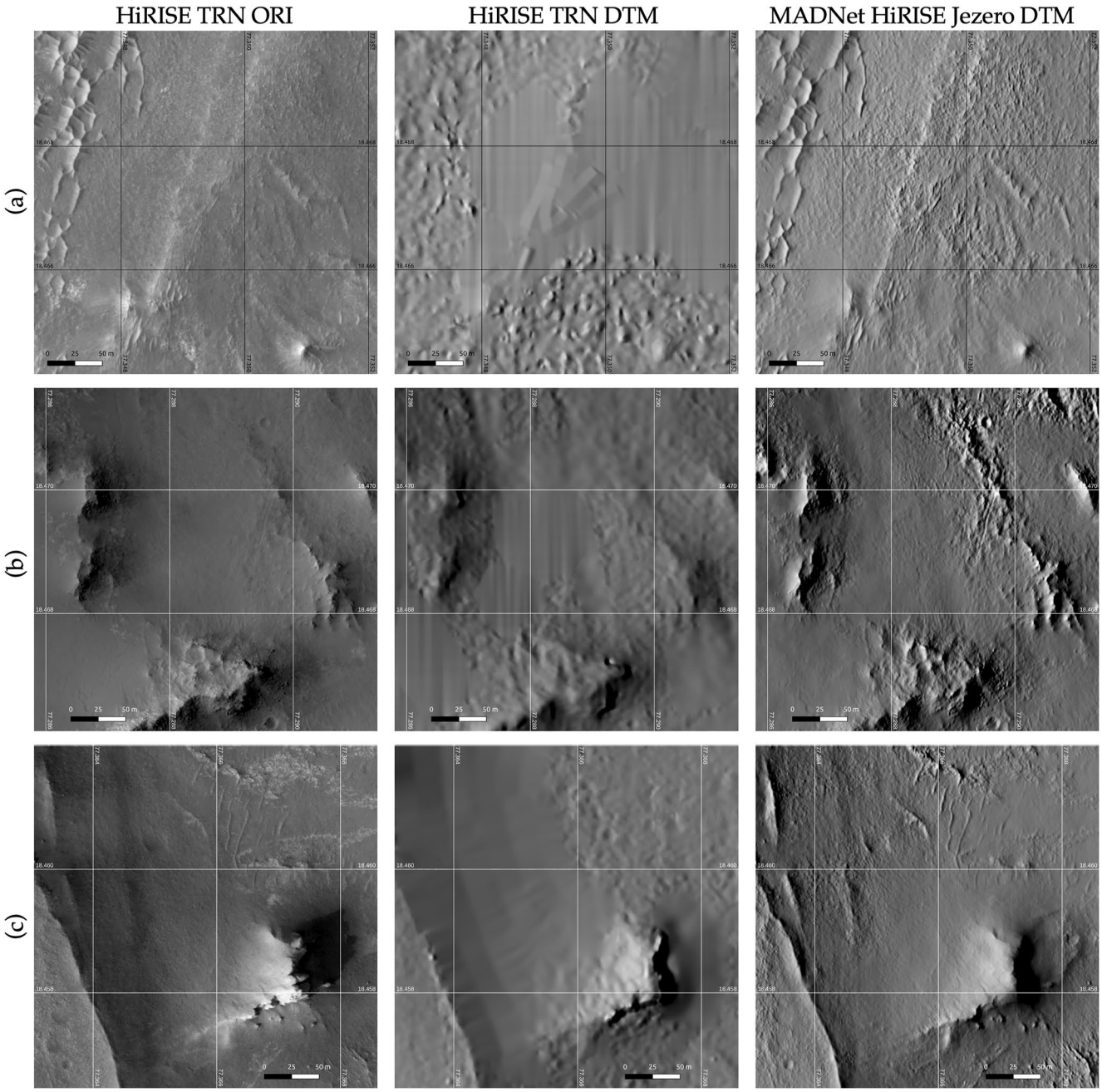


**Figure 6.** Examples of crops of the HiRISE TRN ORI mosaic, shaded relief images (azimuth: 275°; altitude: 30°; vertical exaggeration: (1) of the HiRISE TRN DTM and the refined MADNet HiRISE Jezero DTM, showing interpolation artifacts being eliminated.

and the 463 m/pixel MOLA DTM. The difference maps are shown in Figure 10. The mean and standard deviations of the differences are summarized in Table 3. In general, we observed very good agreement between the MADNet and the originating TRN DTMs, with an average height difference as small as 0.009 m and a standard deviation of 0.63 m. The vertical difference between the MADNet HiRISE DTM mosaic and the CTX TRN DTM mosaic was slightly larger but still had a small mean difference of 0.386 m with a standard deviation of 3.83 m. It should be noted that we can observe some apparent vertical and horizontal stripping as well as contouring artifacts, in Figure 10b, which are originated from the CTX TRN DTMs. It seems that a non-rigid spatial transformation was applied to the CTX TRN DTM, introducing vertical and horizontal interpolation artifacts into the DTM. The same vertical and horizontal stripping artifacts cannot be observed in the MADNet HiRISE DTM mosaic or the corresponding HRSC HMC30 MC-13 DTM.

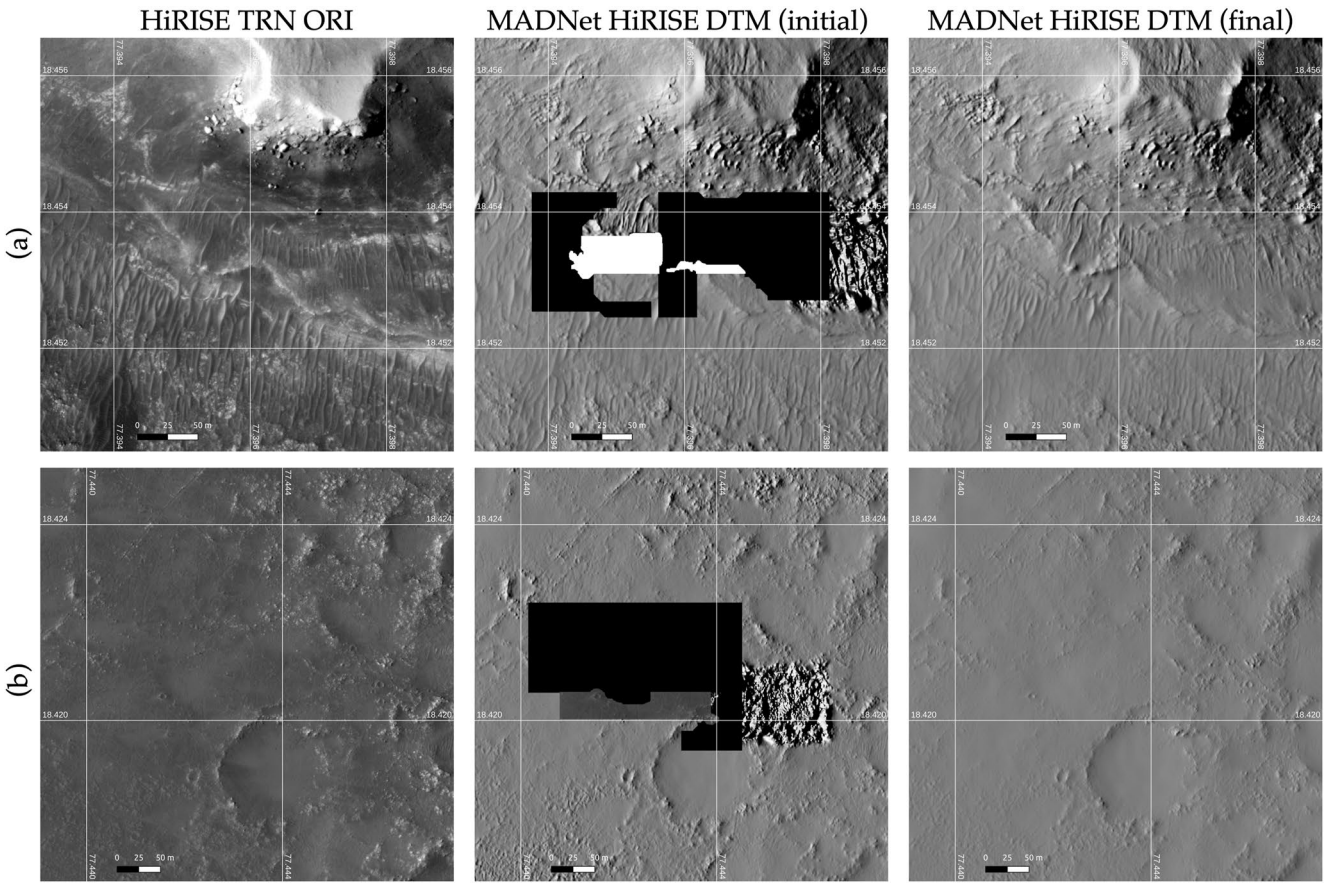


**Figure 7.** Examples of crops of the HiRISE TRN ORI mosaic, shaded relief images (azimuth: 275°; altitude: 30°; vertical exaggeration: (1) of the initial and final version of the refined MADNet HiRISE DTM, showing occasional gaps and artifacts being corrected.

When we compared the MADNet HiRISE DTM to the lower resolution HRSC DTM and the MOLA DTM, we observed much larger vertical differences of up to 3.256 and 21.483 m, respectively, when compared to the differences between the MADNet HiRISE DTM and the higher-resolution CTX and HRSC DTMs. However, as reported in Fergason et al. (2020), the horizontal and vertical accuracies of the HiRISE and CTX TRN DTMs have met and exceeded the standards for TRN. Given that our resultant MADNet HiRISE DTM mosaic is strictly co-aligned with the HiRISE TRN DTM mosaic (with the tiny abovementioned deviations), we did not perform any further co-alignment with respect to the HRSC DTM mosaic or the MOLA DTM.

To avoid interpolation issues associated with the gridded MOLA DTM, a direct comparison is made between the resultant MADNet HiRISE DTM mosaic and the raw MOLA height measurements. These measurements are extracted from the MOLA PDER (Precision Experiment Data Record) products, available at https://pds-geosciences.wustl.edu/missions/mgs/pedr.html, for a rectangular area of 8 km × 8 km at the center of the MADNet HiRISE DTM mosaic. The mean difference and standard deviation between the MADNet HiRISE DTM and the MOLA spots are detailed in Table 3. These values are similar to the mean difference and standard deviation between the MADNet HiRISE DTM and the interpolated MOLA DTM. As previously stated, the comparably larger difference originates from the HiRISE TRN DTM, which was used as the reference DTM for the refinement work.

## 4. Discussion

The resulting MADNet HiRISE DTM mosaic has demonstrated superior performance over the original HiRISE TRN DTM mosaic by USGS in terms of enhanced effective resolution, revealing the topography of fine-scale surface features and eliminating various artifacts. These improvements inevitably result in local differences

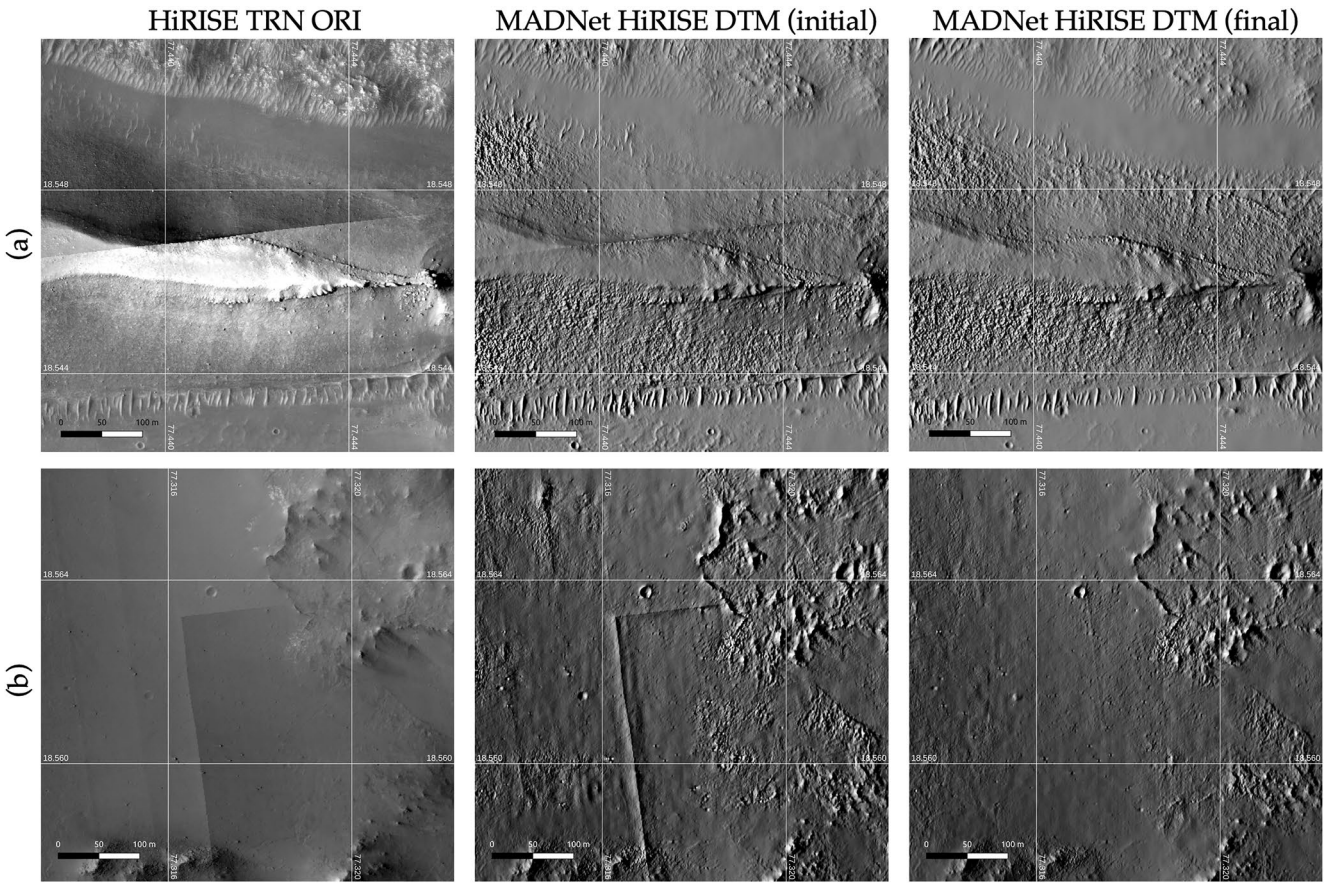


**Figure 8.** Examples of crops of the HiRISE TRN ORI mosaic, shaded relief images (azimuth: 275°; altitude: 30°; vertical exaggeration: (1) of the initial and final version of the refined MADNet HiRISE DTM, showing new striping artifacts caused by the brightness/contrast differences of the neighboring HiRISE images of the input ORI mosaic being corrected.

between the MADNet and the TRN DTM mosaics. Although the averaged overall differences are as small as 0.009 m, the local differences can vary. In theory, if the local differences are too small, then the fine-scale features may not be clearly resolved or may appear blurred. However, if the local differences are too large, then it indicates that the results from the deep learning approach do not agree with the traditional photogrammetric approach. In such cases, additional validation of the correctness will be required using high-resolution ground-truth data, which is currently unavailable for a sufficiently large area on Mars.

To investigate the local differences shown between the MADNet and the original DTM in Figure 10a, we selected two areas (locations are shown in Figure 10a) where large height differences are observed. Zoom-in views and profile measurements of these two areas are shown in Figures 11 and 12, respectively. Figure 11 shows patterned dune features. We can observe that the height differences shown in profile line A–A′ are mainly due to the better reconstruction of the fine-scale features by the MADNet DTM. However, potential overshoot and/or undershoot of these features are likely to exist, but they are likely to be smaller than 5 m for this example region since the maximum height difference found here is less than 5 m. Figure 12 shows a small plateau with small rocks at the edge and craters in the middle. We can observe that the major height differences shown in profile line B-B′ lie at the edges of the two ends of the plateau and the small crater (about 10 m diameter) at the center. The differences are approximately 4, 3, and 6 m at the peak of the north side edge, at the center of the small crater, and at the peak of the south side edge, respectively. These differences are reasonable, considering the different levels of detail resolved in the MADNet and the USGS HiRISE DTMs. However, overshoot and/or undershoot are still likely to exist, but they are considered minor, as shown in this example.

In the future, we plan to compare the MADNet HiRISE DTM mosaic with DTM mosaics from rover data, such as DTMs from Mastcam-Z and Navcam. This comparison will be possible once both sets of data become available

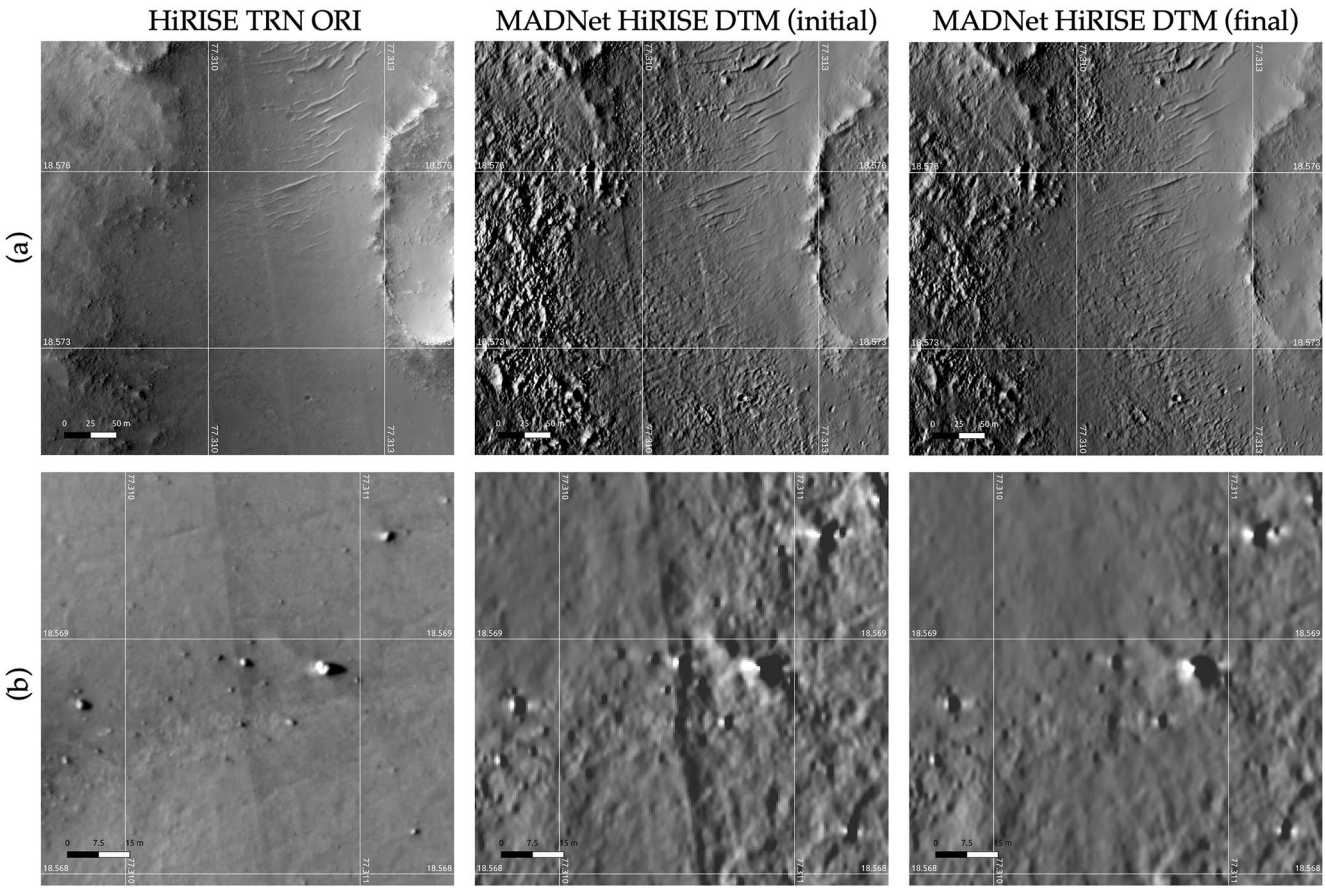


**Figure 9.** Examples of crops of the HiRISE TRN ORI mosaic, shaded relief images (azimuth: 275°; altitude: 30°; vertical exaggeration: (1) of the initial and final version of the refined MADNet HiRISE DTM, showing successful correction of the striping artifacts caused by similar artifacts from the original input single-strip images.

through the VRVis/Joanneum Research's Pro3D® viewer (Paar et al., 2023), in a common global geospatial coordinate system. Currently, we are encountering difficulties in reprojecting and/or matching the rover DTM products available from the PDS site with the HiRISE TRN/MADNet DTMs. Such inter-comparisons will help to evaluate the consistency and accuracy of the MADNet approach and the potential of extending it to other high-resolution data sources.

## 5. Conclusions

In this paper, we present an enhanced 50 cm/pixel HiRISE DTM mosaic of the Mars 2020 landing site at Jezero crater, generated using the MADNet monocular depth estimation network. Our DTM demonstrates significant improvements in effective resolution and artifact elimination over the publicly available USGS Mars 2020 HiRISE TRN ORI and DTM mosaics used as inputs. The resultant MADNet HiRISE Jezero DTM is strictly (0.009 m mean difference with 0.63 m standard deviation) co-aligned with the original HiRISE TRN DTM and ORI mosaics, which are already co-aligned with the USGS CTX-based TRN DTM and ORI mosaics, as well as the HRSC MC-13 DTM and ORI mosaics that cover the same area. We demonstrate each of these improvements with examples and provide quantitative comparisons with respect to other DTM sources. The data are hosted on the FUB server and has been made publicly available http://dx.doi.org/10.17169/refubium-38359.

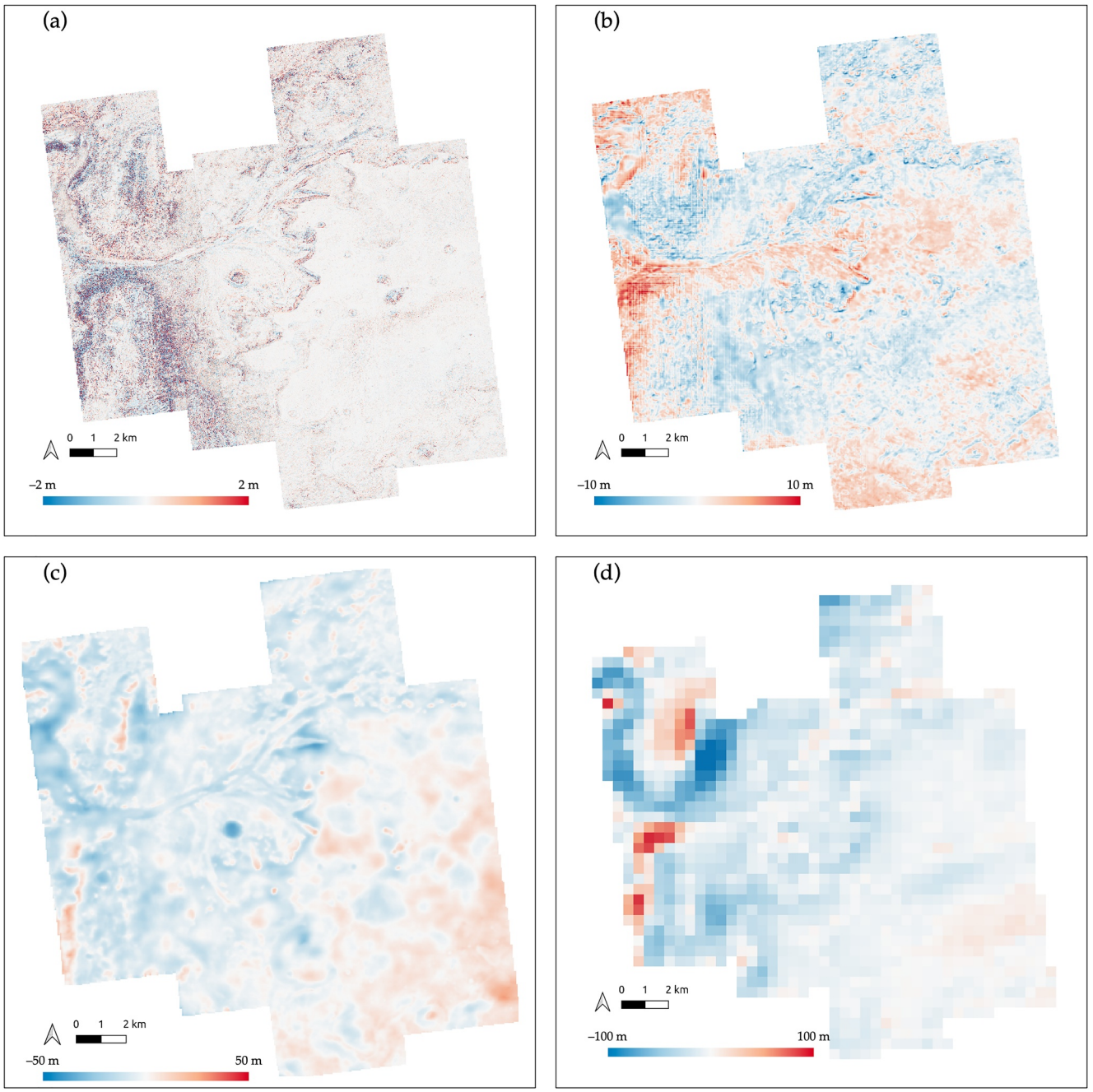


**Figure 10.** Difference maps (a) between the resultant MADNet HiRISE Jezero DTM mosaic and the originating HiRISE TRN DTM mosaic at 1 m/pixel for the comparison; (b) between the resultant MADNet HiRISE Jezero DTM mosaic and the CTX TRN DTM mosaic at 20 m/pixel for the comparison; (c) between the resultant MADNet HiRISE Jezero DTM mosaic and the HMC30 MC-13 DTM at 50 m/pixel for the comparison; and (d) between the resultant MADNet HiRISE Jezero DTM mosaic and the MOLA DTM at 463 m/pixel for the comparison. The two areas (Area-A and Area-B) that are identified with larger differences between the HiRISE MADNet and TRN DTMs are labeled in subfigure (a) for the follow-up profile measurements.

**Table 3**
*Summary of the Mean and Standard Deviations of the Differences Between the Resultant MADNet HiRISE Jezero DTM, the Originating HiRISE TRN DTM Mosaic, the CTX TRN DTM Mosaic, the HRSC HMC_13E10 DTM, the MOLA DTM and the MOLA Points*

| Comparison inputs | | Comparison resolution | Mean difference (m) | Standard deviation (m) |
|---|---|---|---|---|
| MADNet HiRISE Jezero DTM | HiRISE TRN DTM | 1 m/pixel | 0.009 | 0.63 |
| | CTX TRN DTM | 20 m/pixel | −0.386 | 3.83 |
| | HMC30 13E DTM | 50 m/pixel | −3.256 | 18.83 |
| | Mars MGS MOLA DTM 463m v2 | 463 m/pixel | −21.483 | 42.13 |
| | Mars MGS MOLA points | n/a | −18.252 | 36.44 |

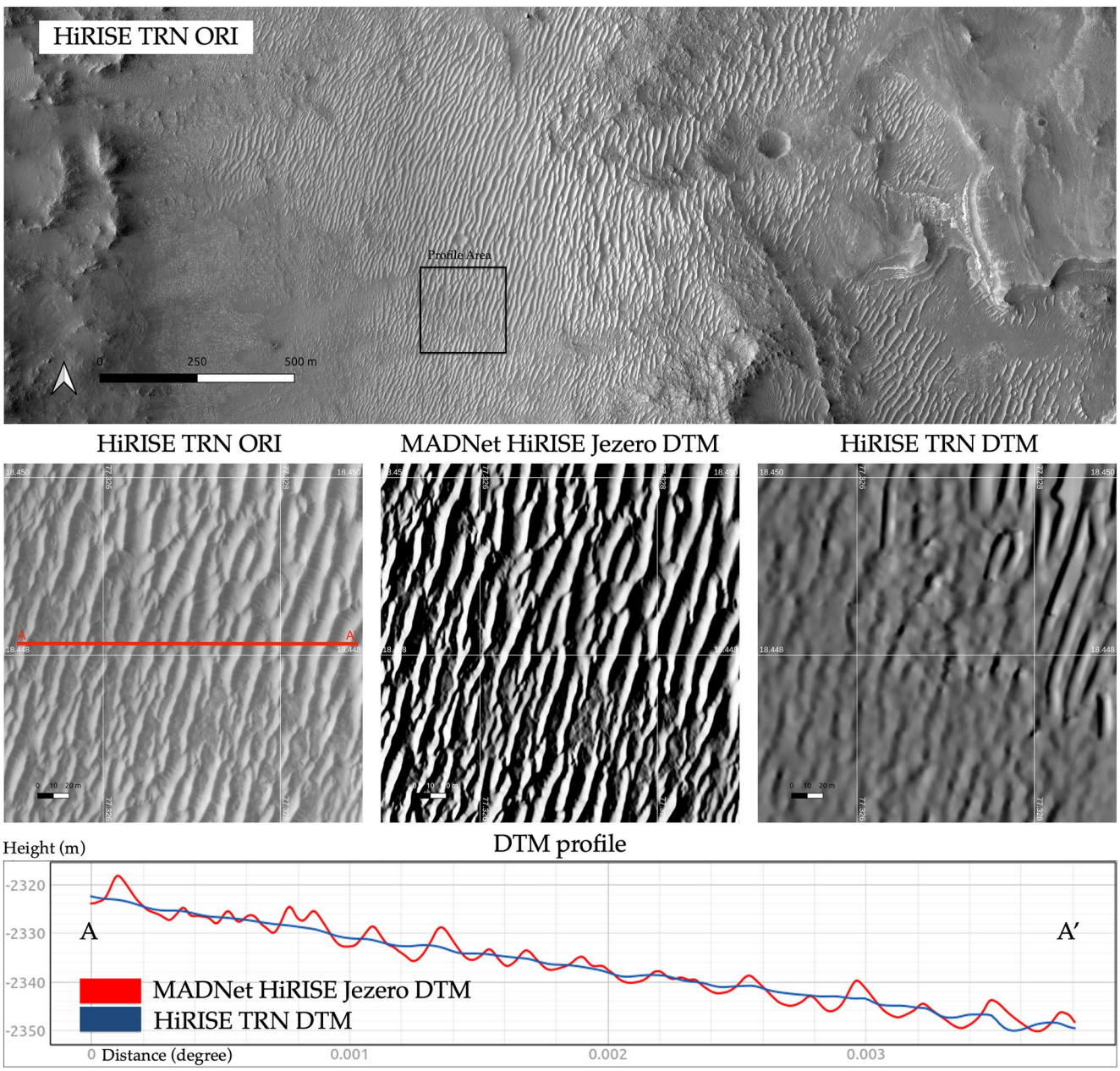


**Figure 11.** Examples of crops of the HiRISE TRN ORI mosaic, shaded relief images (azimuth: 275°; altitude: 30°; vertical exaggeration: (1) of the MADNet and HiRISE TRN DTM mosaics, and profile measurements, over one of the selected areas where large height difference between the MADNet and HiRISE TRN DTM mosaics are shown (Area-A of Figure 10a).

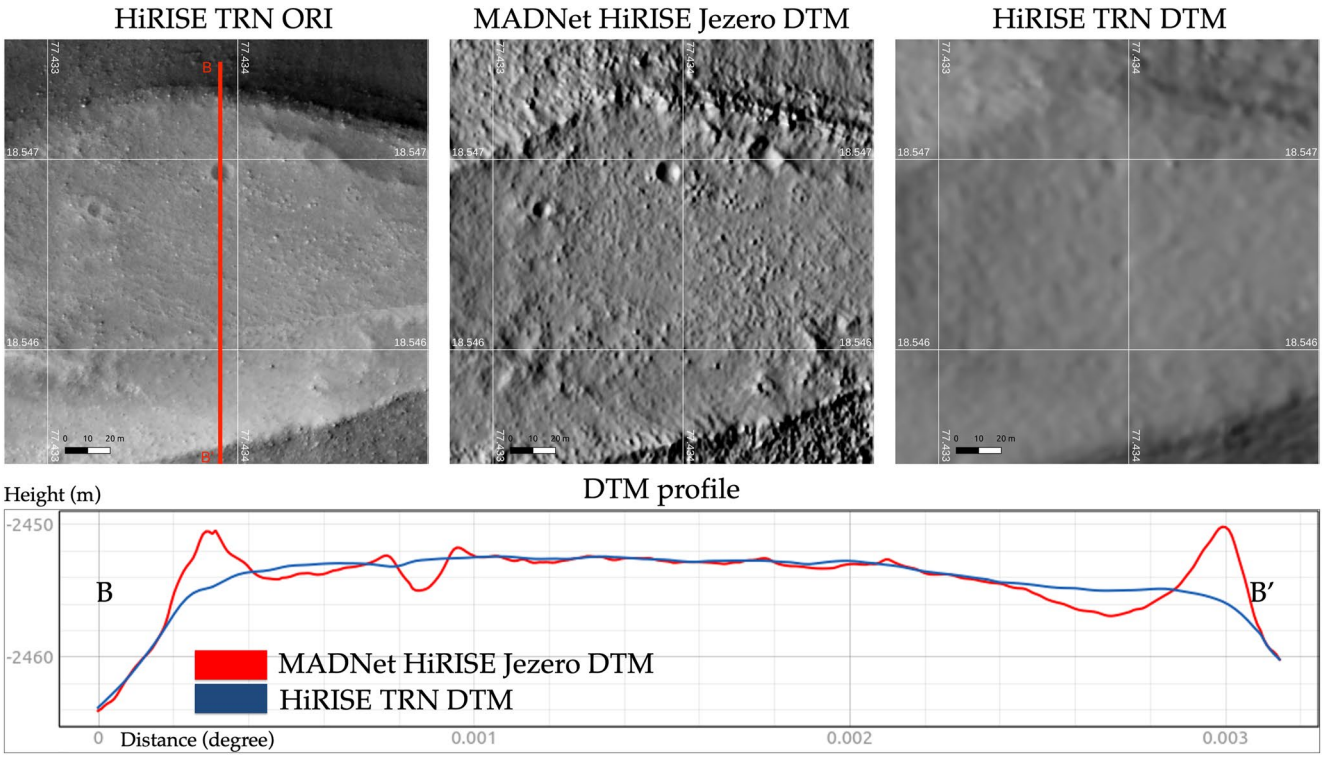


**Figure 12.** Examples of crops of the HiRISE TRN ORI mosaic, shaded relief images (azimuth: 275°; altitude: 30°; vertical exaggeration: (1) of the MADNet and HiRISE TRN DTM mosaics, and profile measurements, over one of the selected areas where large height difference between the MADNet and HiRISE TRN DTM mosaics are shown (Area-B of Figure 10a).

## Data Availability Statement

The resultant data products are publicly available on the FUB server at http://dx.doi.org/10.17169/refubium-38359 (under CC BY 4.0 license).

**Acknowledgments**
This work is supported by the German Space Agency (DLR Bonn), Grant 50 OO 2204 (Koregistrierung), on behalf of the German Federal Ministry for Economic Affairs and Climate Action. Initial development work of the MADNet network was funded by the UKSA Aurora program (2018–2021) under Grant ST/S001891/1 at UCL. Open Access funding enabled and organized by Projekt DEAL.

## References

Fergason, R. L., Hare, T. M., Mayer, D. P., Galuszka, D. M., Redding, B. L., Smith, E. D., et al. (2020). Mars 2020 terrain relative navigation flight product generation: Digital terrain model and orthorectified image mosaic. In *51st annual lunar and planetary science conference*. (No. 2326).

Goodfellow, I. J., Pouget-Abadie, J., Mirza, M., Xu, B., Warde-Farley, D., Ozair, S., et al. (2014). Generative adversarial networks. *arXiv, arXiv:1406.2661*.

Gwinner, K., Jaumann, R., Hauber, E., Hoffmann, H., Heipke, C., Oberst, J., et al. (2016). The High Resolution Stereo Camera (HRSC) of Mars Express and its approach to science analysis and mapping for Mars and its satellites. *Planetary and Space Science*, *126*, 93–138. https://doi.org/10.1016/j.pss.2016.02.014

Gwinner, K., Scholten, F., Spiegel, M., Schmidt, R., Giese, B., Oberst, J., et al. (2009). Derivation and validation of high-resolution digital terrain models from Mars Express HRSC data. *Photogrammetric Engineering & Remote Sensing*, *75*(9), 1127–1142. https://doi.org/10.14358/pers.75.9.1127

Huang, G., Liu, Z., Van Der Maaten, L., & Weinberger, K. Q. (2017). Densely connected convolutional networks. In *Proceedings of the IEEE conference on computer vision and pattern recognition* (pp. 4700–4708).

Jolicoeur-Martineau, A. (2018). The relativistic discriminator: A key element missing from standard GAN. *arxiv, arXiv:1807.00734*.

Laina, I., Rupprecht, C., Belagiannis, V., Tombari, F., & Navab, N. (2016). Deeper depth prediction with fully convolutional residual networks. In *Proceedings of the 2016 fourth international conference on 3D vision (3DV)* (pp. 239–248).

Malin, M. C., Bell, J. F., Cantor, B. A., Caplinger, M. A., Calvin, W. M., Clancy, R. T., et al. (2007). Context camera investigation on board the Mars Reconnaissance Orbiter. *Journal of Geophysical Research*, *112*(E5), 112. https://doi.org/10.1029/2006je002808

Mangold, N., Dromart, G., Ansan, V., Salese, F., Kleinhans, M. G., Massé, M., et al. (2020). Fluvial regimes, morphometry, and age of Jezero crater paleolake inlet valleys and their exobiological significance for the 2020 Rover Mission Landing Site. *Astrobiology*, *20*(8), 994–1013. https://doi.org/10.1089/ast.2019.2132

McEwen, A. S., Eliason, E. M., Bergstrom, J. W., Bridges, N. T., Hansen, C. J., Delamere, W. A., et al. (2007). Mars reconnaissance orbiter's high resolution imaging science experiment (HiRISE). *Journal of Geophysical Research*, *112*(E5), E05S02. https://doi.org/10.1029/2005je002605

Neukum, G., & Jaumann, R. (2004). HRSC: The high resolution stereo camera of Mars Express. *Scientific Payloads*, *1240*, 17–35.

Neumann, G. A., Rowlands, D. D., Lemoine, F. G., Smith, D. E., & Zuber, M. T. (2001). Crossover analysis of Mars Orbiter Laser Altimeter data. *Journal of Geophysical Research*, *106*(E10), 23753–23768. https://doi.org/10.1029/2000je001381

Paar, G., Ortner, T., Tate, C., Deen, R. G., Abercrombie, P., Vona, M., et al. (2023). Three-dimensional data preparation and immersive mission-spanning visualization and analysis of Mars 2020 Mastcam-Z stereo image sequences. *Earth and Space Science*, *10*(3), e2022EA002532. https://doi.org/10.1029/2022ea002532

Ronneberger, O., Fischer, P., & Brox, T. (2015). U-net: Convolutional networks for biomedical image segmentation. In *Proceedings of the international conference on medical image computing and computer-assisted intervention* (pp. 234–241).

Sidiropoulos, P., Muller, J. P., Watson, G., Michael, G., & Walter, S. (2018). Automatic coregistration and orthorectification (ACRO) and subsequent mosaicing of NASA high-resolution imagery over the Mars MC11 quadrangle, using HRSC as a baseline. *Planetary and Space Science*, *151*, 33–42. https://doi.org/10.1016/j.pss.2017.10.012

Smith, D. E., Zuber, M. T., Frey, H. V., Garvin, J. B., Head, J. W., Muhleman, D. O., et al. (2001). Mars orbiter laser altimeter—Experiment summary after the first year of global mapping of Mars. *Journal of Geophysical Research*, *106*(E10), 23689–23722. https://doi.org/10.1029/2000je001364

Stack, K. M., Williams, N. R., Calef, F., Sun, V. Z., Williford, K. H., Farley, K. A., et al. (2020). Photogeologic map of the perseverance rover field site in Jezero Crater constructed by the Mars 2020 Science Team. *Space Science Reviews*, *216*(8), 1–47. https://doi.org/10.1007/s11214-020-00739-x

Tao, Y., Muller, J. P., Xiong, S., Conway, S. J., Guimpier, A., Fawdon, P., et al. (2021b). Rapid single image-based DTM estimation from ExoMars TGO CaSSIS images using generative adversarial U-Nets. *Remote Sensing*, *13*(15), 2877. https://doi.org/10.3390/rs13152877

Tao, Y., Muller, J. P., Xiong, S., Conway, S. J., Putri, A. R. D., Walter, S. H. G., et al. (2018). Massive stereo-based DTM production for Mars on cloud computers. *Planetary and Space Science*, *154*, 30–58. https://doi.org/10.1016/j.pss.2018.02.012

Tao, Y., Xiong, S., Conway, S. J., Muller, J. P., Michael, G., Cremonese, G., & Thomas, N. (2022). Subpixel-scale topography retrieval of Mars using single-image DTM estimation and super-resolution restoration. *Remote Sensing*, *14*(2), 257. https://doi.org/10.3390/rs14020257

Tao, Y., Xiong, S., Muller, J. P., & Conway, S. J. (2021c). Large area high-resolution 3D mapping of Oxia Planum: The landing site for the ExoMars Rosalind Franklin rover. *Remote Sensing*, *13*(16), 3270. https://doi.org/10.3390/rs13163270

Tao, Y., Xiong, S., Muller, J. P., Conway, S. J., Michael, G., Cremonese, G., & Thomas, N. (2021a). MADNet 2.0: Pixel-scale topography retrieval from single-view orbital imagery of Mars using deep learning. *Remote Sensing*, *13*(21), 4220. https://doi.org/10.3390/rs13214220

Zwald, L., & Lambert-Lacroix, S. (2012). The berhu penalty and the grouped effect. *arXiv, arXiv:1207.6868*.